Available online at www.sciencedirect.com
ScienceDirect
Journal of Nuclear Materials 377 (2008) 59–64
journal of nuclear materials
www.elsevier.com/locate/jnucmat

Thermal stability of nano-structured ferritic alloy

P. Miao *, G.R. Odette, T. Yamamoto, M. Alinger, D. Klingensmith

Department of Mechanical Engineering, University of California, Santa Barbara, CA 93106-5080, USA

Abstract

The excellent tensile and creep strength and the potential for managing radiation damage make nano-structured ferritic alloys (NFAs) promising candidates for high-temperature applications in spallation proton, advanced fission and fusion neutron environments. The thermal stability of NFAs is critical for such applications, hence, this has been investigated in a series of aging experiments on MA957 at 900 °C, 950 °C and 1000 °C for times up to 3000 h. Optical and transmission electron microscopy (TEM) studies showed the fine scale grain and dislocation structures are stable up to 1000 °C. TEM and small angle neutron scattering (SANS) showed that the nm-scale solute cluster-oxide features (NFs), that are a primary source of the high strength of NFAs, were stable at 900 °C and coarsened only slightly at 950 °C and 1000 °C. Porosity that developed during high-temperature aging was minimal at 900 °C and modest at 950 °C, but was much larger after 1000 °C. Microhardness was basically unchanged after the 900 °C aging, and decreased only slightly ($\leqslant$3%) after aging at 950 °C and 1000 °C.

PACS: 61.46.−w; 61.46.Df; 81.40.−z; 81.20.Ev

1. Introduction

Nano-structured ferritic alloys (NFAs) have outstanding low-temperature tensile and high-temperature creep strength [1–9] and potential for managing radiation damage [1,10,11], including high helium levels in fusion and advanced fission neutron as well as spallation proton environments. The excellent properties of NFAs primarily derive from a high density of nm-sized Y–Ti–O precipitate cluster and/or complex oxides, such as $Y_2Ti_2O_7$ and Y_2TiO_5, that form during hot consolidation following mechanical alloying [1,7,12–18]. The nanofeatures (NFs) are reported to be stable, at least for a limited range of irradiation conditions [1,10,19–21]. A key issue for NFAs is stability of their excellent properties and microstructures at high-temperatures.

The high-temperature and short-time thermal stability of NFAs were previously investigated in a series of aging experiments of MA957 at 1150–1400 °C for various times ranging from 1/3 to 480 h. These experiments showed significant coarsening of the NFs, rapid growth of porosity and large decrease of microhardness with increasing aging temperature and time [7,12]. However, the aging temperatures in these experiments were much higher than those are expected for application of NFAs in the range from ≈650 to 850 °C. Indeed, fits of kinetic coarsening models yielded parameters to the high-temperature aging data predicted very high NF stability at lower temperatures. Based on the aging data covering the initial period of coarsening, at NF sizes less than 5–6 nm, yielded activation energies in excess of 850 kJ/mol and a $t^{1/5}$ time-dependence [7,12]. Atom probe tomography studies have also suggested that the NFs are remarkably stable at high-temperature and during creep [17,22]. Thus, to confirm these observations, we initiated a series of aging experiments of MA957 at temperatures from 800 to 1000 °C for planned times up to 20 000 h or more. Interim results on the effects of aging at 900 °C, 950 °C and 1000 °C up to 3000 h are reported here.

* Corresponding author. Tel.: +1 805 893 3848; fax: +1 805 893 4731.
E-mail address: p.miao@engineering.ucsb.edu (P. Miao).

0022-3115/$ - see front matter © 2008 Elsevier B.V. All rights reserved.
doi:10.1016/j.jnucmat.2008.02.042

2. Experimental

Coupon specimens of as-received MA957 alloy extruded at 1150 °C with a nominal composition of Fe–14 wt% Cr, 0.9% Ti, 0.3% Mo, and 0.25% Y_2O_3 were thermally aged for 3000 h at 900 °C, 950 °C and 1000 °C in quartz capsules which were vacuum evaporated and backfilled with dry helium at 50 kPa.

The coarser scale and NF microstructures of the as-extruded and the aged MA957 were characterized using optical microscopy, TEM (JEOL2010HR) and SANS (NG7 at the National Institute of Standards and Technology). Standard 3 mm TEM discs, taken from a region of ≈1 mm away from sample surface, were ground to a thickness of ≈0.15 mm and then thinned to electron transparency in a TENUPOL twin-jet electro-polisher with $H_2SO_4 + 80\%CH_3OH$ at room temperature. The thinned samples were carefully washed in methanol, transformed to a vacuum desiccator and then loaded to TEM for observation within one hour to minimize contamination. TEM images for the measurement of the NFs were taken in a near [0 1 1] orientation. The thickness of the TEM samples was measured by the convergent beam diffraction technique. Details of the experiment, data reduction and analysis for SANS are given elsewhere [7].

Mechanical properties of the MA957 samples were evaluated by Vickers microhardness at a 500 g load.

3. Results

As shown in the TEM micrographs in Figs. 1 and 2 in a region ≈1 mm away below the sample surface, the as-extruded MA957 has fine ferrite grains and a high dislocation density (Figs. 1a and 2a) that remain stable after 3000 h aging at 900 °C, 950 °C and 1000 °C (Figs. 1b, c, d and 2b, c, d). The ferrite grain sizes and dislocation density are unchanged after aging. Note that ferrite grains in a very thin layer (⩽30 μm for 950 °C and ⩽200 μm for 1000 °C) close to the sample surfaces coarsened at 950 °C and 1000 °C. Composition analysis of these regions indicates that the local coarsening is due to the sublimation of the elements like Cr. Thus protection coatings, like alumina scale, will be needed to use NFAs at temperatures higher than 900 °C in environments such as helium coolants.

The as-extruded and the aged MA957 have a large number of NFs, as seen in Fig. 3. Their diameter (d), number density (N) and volume fraction (f) were measured based on computer assisted image analysis of TEM micrographs and convergent beam estimates of the foil thickness. These data are shown in Figs. 4 and 5. Large particles, with diameters greater than ≈10 nm, were not included in the measurements. The average diameters are 2.1 ± 0.4, 2.1 ± 0.4, 2.6 ± 0.5 and 3.1 ± 0.9 nm for the as-extruded and the 900 °C, 950 °C and 1000 °C aged MA957, respectively. The corresponding total number density of NF after

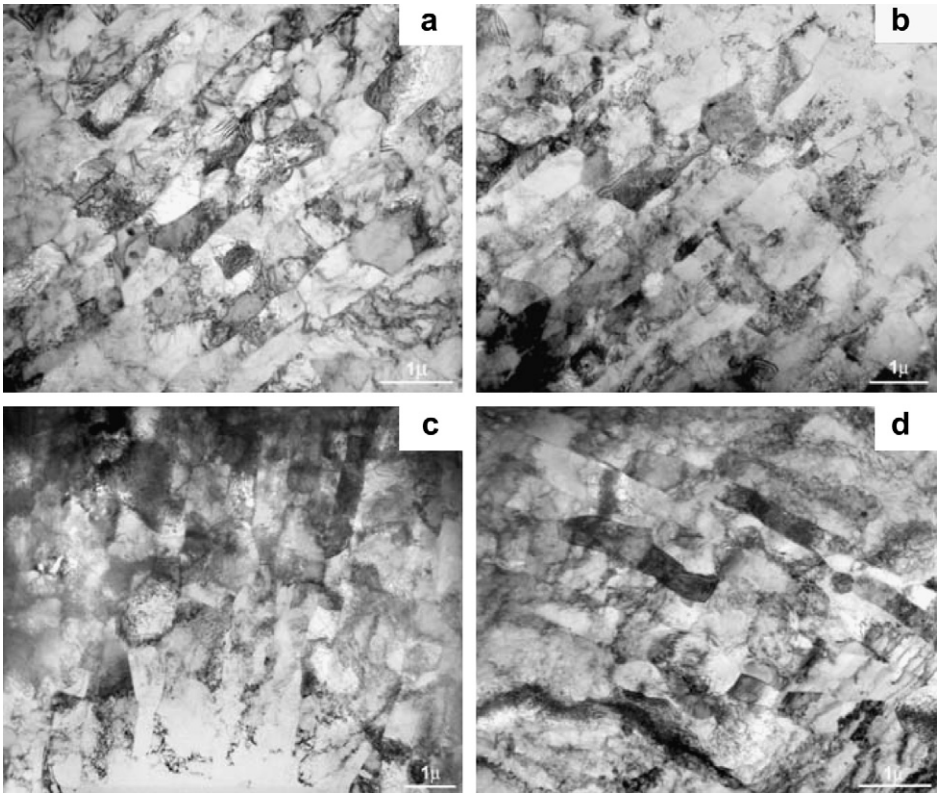

Fig. 1. TEM micrographs of (a) the as-extruded MA957 and (b) 900 °C, (c) 950 °C and (d) 1000 °C aged MA957.

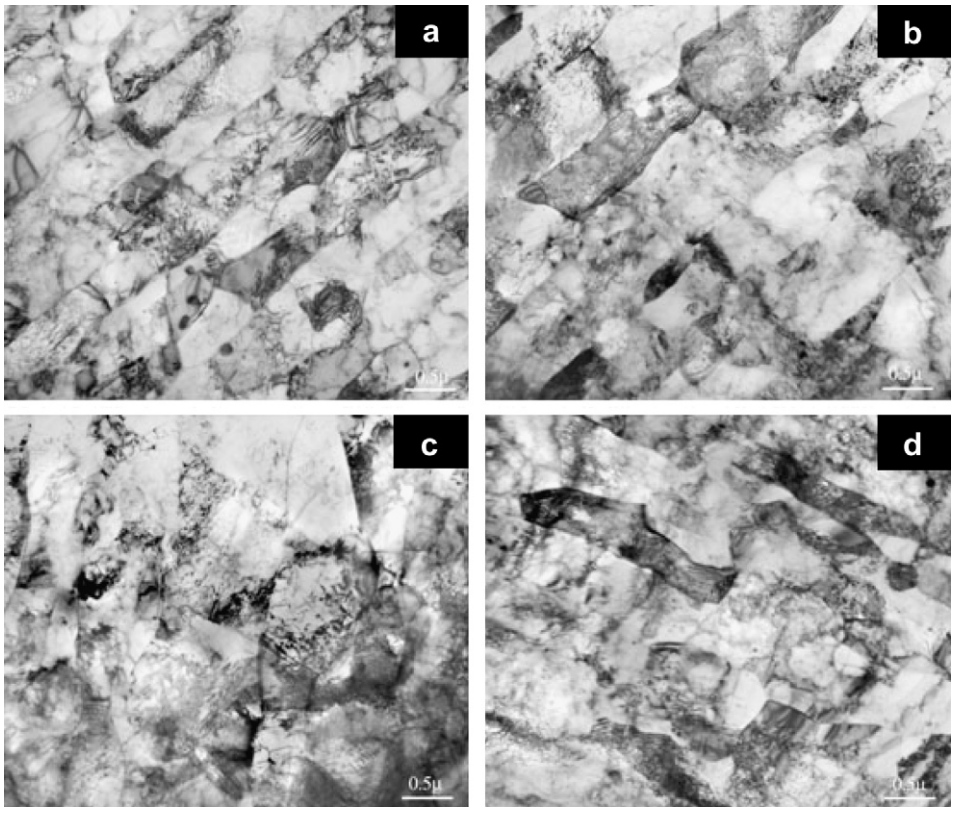

Fig. 2. Higher magnification of Fig. 1, showing dislocations in (a) the as-extruded MA957 and (b) 900 °C, (c) 950 °C and (d) 1000 °C aged MA957.

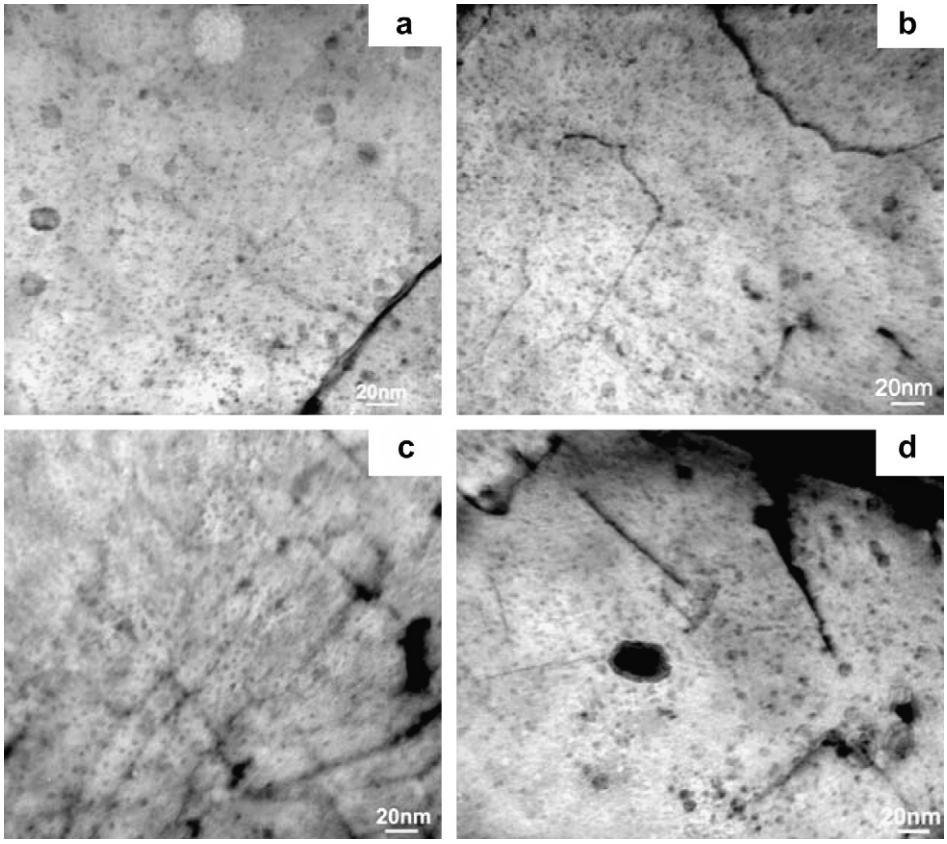

Fig. 3. NFs in (a) the as-extruded MA957 and (b) 900 °C, (c) 950 °C and (d) 1000 °C aged MA957.

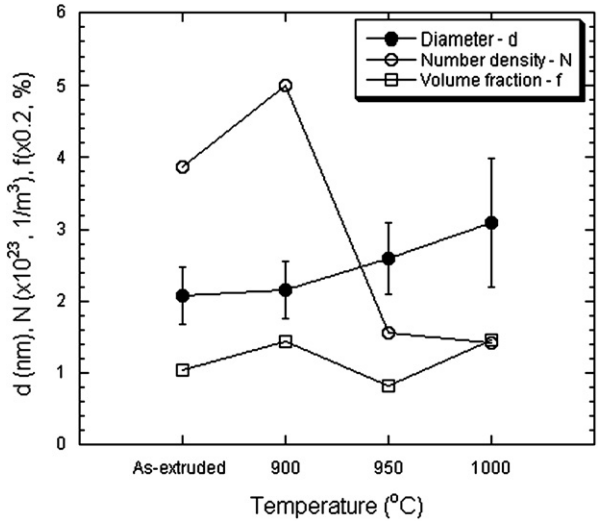

Fig. 4. Average diameter, total number density and volume fraction of NFs in the as-extruded and aged MA957.

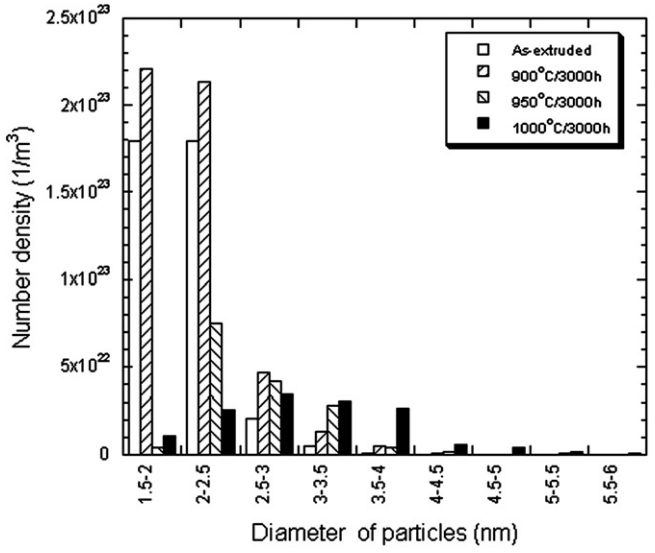

Fig. 5. Number density distribution of NFs in the as-extruded and aged MA957.

900 °C aging is similar to that for the as-extruded MA957, within the uncertainties associated with single area measurements, resolution limits and other possible sources of error. However, the number densities of NF decrease significantly after 950 °C and 1000 °C aging. Nevertheless, the total volume fraction did not change significantly. Note these evaluations are in good qualitative agreement with measurements by SANS, but the d was about 20% smaller and the N and f are 40% and 50% higher, respectively, for the TEM measurements. The absence of coarsening at 900 °C, which does occur at 950 °C and 1000 °C, is more clearly shown in the number density distribution histograms presented in Fig. 5. The NF distributions at 900 °C are nearly the same as those in the as-extruded, but they shift to larger diameters at 950 °C and even more so at 1000 °C.

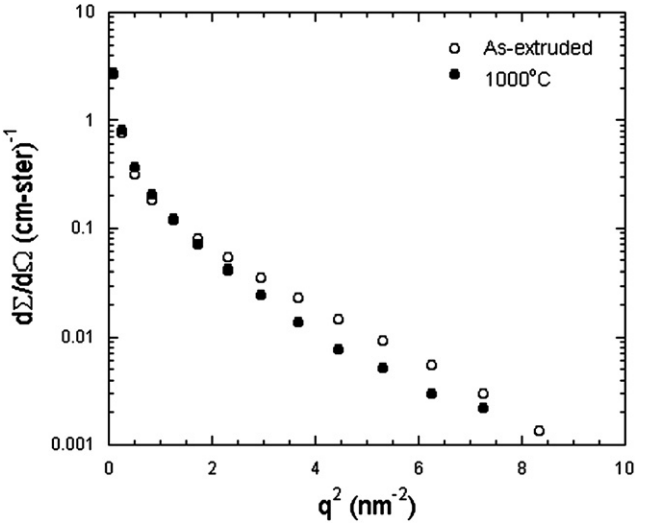

Fig. 6. SANS cross-section curves at a 45° angle to the direction of the magnetic field.

The NF coarsening at 1000 °C was also qualitatively confirmed by the SANS experiment, as shown in Fig. 6. The open and filled symbols are the NF scattering cross-sections measured at 45° to the magnetic field (this includes the nuclear plus 50% of the magnetic scattering) as a function of the square of the scattering vector, q, for the as-extruded and 1000 °C–3000 h aged conditions, respectively. The decrease in the magnitude of $d\Sigma/d\Omega$ vs. q^2 for 1000 °C-aged MA957 at higher q and increase at very low q in the aged condition indicates a slight coarsening of the NFs.

Porosities of the as-extruded and the aged MA957 were measured from optical micrographs of as-polished cross-sections normal to the extrusion as shown in Table 1 and illustrated in Fig. 7. The pore diameters and area fractions increased ≈25% and 200%, respectively, after aging at 900 °C and 950 °C, respectively. Much of this increase is due to the growth of pores that are visible in the as-received condition; however, as indicated in Table 1, the pore density may also increase slightly due to the growth of previously invisible submicron-sized pores [23] formed during mechanical alloying. The average diameter and area fraction of the pores grow much more significantly after aging at 1000 °C, with increases of ≈350% and 1150%, respectively. The apparent decrease in the number density of pores may be due to coalescence.

Vicker's diamond pyramid hardness (DPH, kg/mm^2) measurements on polished cross-sections parallel to the

Table 1
Average diameter, area fraction and number density of pores

Heat treatment	Average diameter of pores (μm)	Area fraction of pores (%)	Number density of pores ($\times 10^9$, 1/m^2)
As-extruded	2.2 ± 1.2	0.5	1.0
900 °C/3000 h	2.8 ± 2.4	1.5	1.4
950 °C/3000 h	2.7 ± 2.5	1.2	1.1
1000 °C/3000 h	10.1 ± 8.7	6.2	0.5

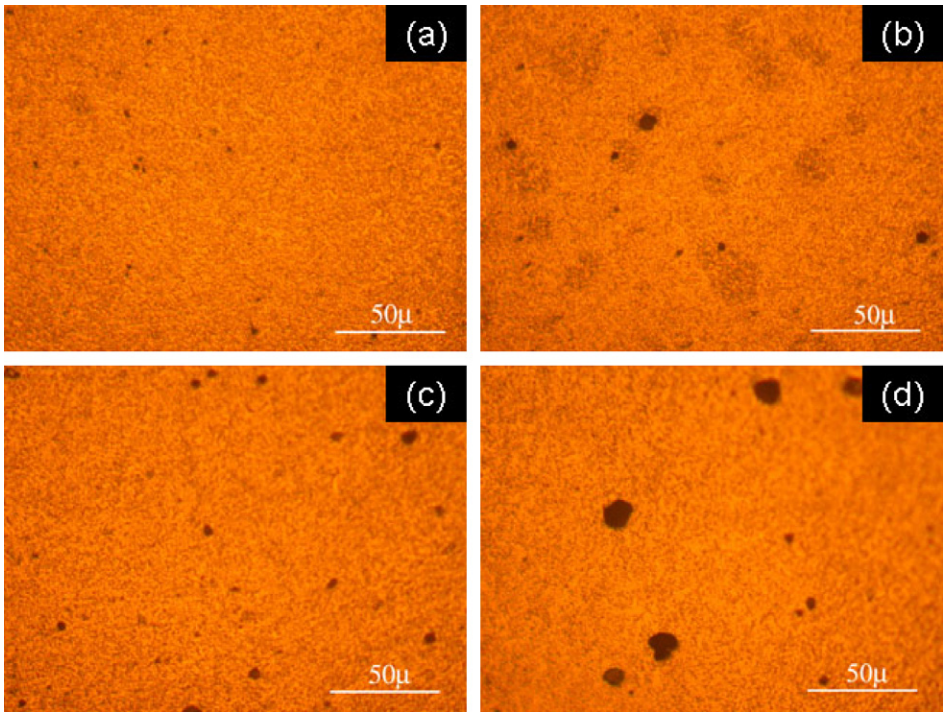

Fig. 7. Optical micrographs in cross-sections normal to the extrusion direction of (a) the as-extruded MA957 and (b) 900 °C, (c) 950 °C and (d) 1000 °C aged MA957. Note that the black features in (a)–(d) are pores.

Table 2
DPH of as-extruded and aged MA957

Heat treatment	As-extruded	900 °C/3000 h	950 °C/3000 h	1000 °C/3000 h
DPH	333 ± 8	332 ± 7	323 ± 7	330 ± 6

extrusion direction are shown in Table 2. The measurements were made at ≈1 mm depth, which is sufficient to avoid the artifacts associated with the near surface environmentally induced instabilities noted above. Slight softening is observed after aging but is insignificant (<1%) except perhaps at 950 °C, where the DPH decreases by ≈3%. However, given the one standard deviation uncertainties in the hardness of ≈±6 to 8 DPH, it is concluded that softening after aging is minimal to non-existent.

4. Discussion

The SANS investigation [7] of MA957 after high-temperature (1150–1250 °C) and short-time (1/3–480 h) aging showed significant NF coarsening. The data in the initial coarsening regime for aging at 1150–1250 °C for 1/3–480 h were least square fitted using expression with the form

$$d(T,t) = d_0[tk'_{co}\exp(-Q_{ec}/RT) + 1]^p. \quad (1)$$

Here d_0 and $d(T,t)$ are the NF sizes before and after aging, respectively, t is the aging time, T is the aging temperature (K), and R is the gas constant. The fits yielded a rate coefficient, $k'_{co} = 2.94 \times 10^{27}$ s^{-1}, an effective activation energy for coarsening, $Q_{ec} \approx 884$ kJ/mol, and a time scaling exponent, $p = 0.2$. The fitted p is consistent with a dislocation pipe diffusion mechanism, but the rather remarkably high value of Q_{ec} is not well understood. Assuming a $d_0 = 2.6$ nm for the as-extruded MA957 based on SANS measurement [7], predictions of Eq. (1) for high-temperature aging for 3000 h are shown by the open circles in Fig. 8, along with the longest time data from the previous high-temperature aging study. Extrapolations of Eq. (1)

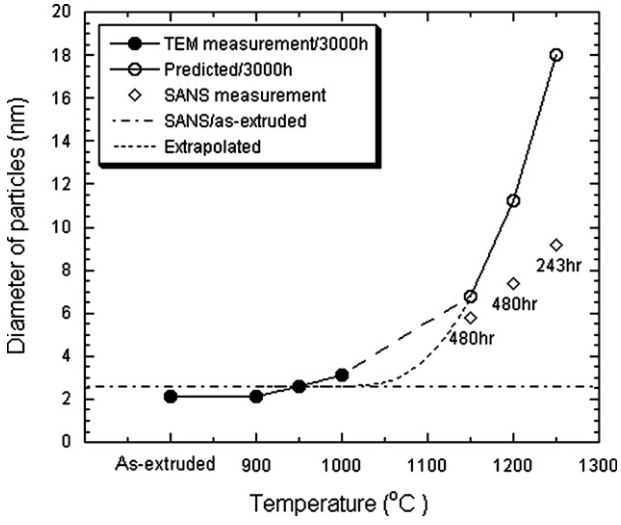

Fig. 8. Size variation of NFs with temperature for the as-extruded and the aged MA957. The filled circles: NF sizes measured by TEM, the open diamonds: NF sizes measured by SANS, and the open circles: NF sizes predicted using Eq. (1) for 1150 °C/3000 h, 1200 °C/3000 h and 1250 °C/3000 h aging.

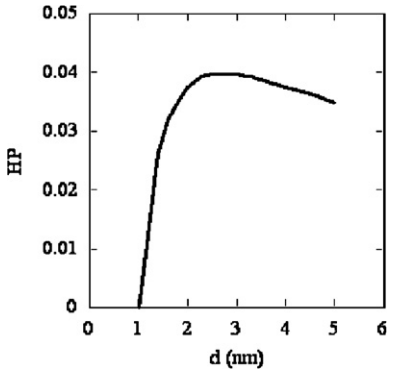

Fig. 9. Variation of hardening parameter (HP) with the NF size (d).

to lower temperatures predict insignificant coarsening below ≈1050 °C. Thus the high-temperature aging model is somewhat inconsistent with the current lower temperature results at 950 °C and 1000 °C. While the coarsening is modest even at 1000 °C, and does not lead to significant softening, data at longer times will be needed to refine the aging model for predicting thermal stability in the application regime for NFAs below ≈850 °C.

The small hardness change is consistent with previous estimates of the relation between the strengthening contribution of the NFs and their corresponding d and f [7]. This work showed that the individual NF contribution to the yield stress is proportional to $\mathrm{HP} = \log(d/4b)b/d$, where HP is a hardening parameter and b is the Burgers vector (0.25 nm) for Fe. Fig. 9 shows that the HP plotted versus d has a broad maximum, peaking around $d \approx 2.5$ nm; the predicted HP actually increases slightly between $d = 2$ and 2.5 nm and is almost constant between $d = 2.5$ and 3 nm.

5. Summary and conclusions

The interim MA957 aging data show that the fine ferrite grains and high dislocation densities are thermally stable at 900 °C, 950 °C and 1000 °C for 3000 h. The NFs are thermally stable at 900 °C, but coarsen slightly at 950 °C and 1000 °C. However the NF coarsening did not lead to significant softening, consistent with expectation. The growth porosity is much smaller at 900 °C and 950 °C compared with the 1000 °C aging.

Acknowledgements

This research was supported by the NERI DOE Office of Nuclear Energy (Grant #DE-FC07-05ID14663) and the DOE Office of Fusion Energy Science (Grant #DE-FG03-94ER54275). The outstanding support for the SANS experiments provided by the NIST Center for Neutron Research is also gratefully acknowledged.

References

[1] M.L. Hamilton, D.S. Gelles, R.J. Lobsinger, G.D. Johnson, W.F. Brown, M.M. Paxton, R.J. Puigh, C.R. Eiholzer, M.A. Blotter, Fabrication Technological Development of the Oxide Dispersion Strengthened Alloy MA957 for Fast Reactor Applications, PNNL-13168 (released 2000), 1991.
[2] C. Zakine, C. Prioul, D. Francois, Mater. Sci. Eng. A 219 (1996) 102.
[3] S. Ukai, T. Okuda, M. Fujiwara, T. Kobayashi, S. Mizuta, H. Nakashima, J. Nucl. Sci. Technol. 39 (8) (2002) 872.
[4] S. Ukai, M. Fujiwara, J. Nucl. Mater. 307–311 (2002) 749.
[5] M.J. Alinger, G.R. Odette, G.E. Lucas, J. Nucl. Mater. 307–311 (2002) 484.
[6] R.L. Klueh, P.J. Maziasz, I.S. Kim, L. Heatherly, D.T. Hoelzer, N. Hashimoto, E.A. Kenik, K. Miyahara, J. Nucl. Mater. 307–311 (2002) 773.
[7] M.J. Alinger, On the Formation and Stability of Nanometer Scale Precipitates in Ferritic Alloys during Processing and High Temperature Service, PhD thesis, University of California, Santa Barbara, 2004.
[8] A. Alamo, V. Lambard, X. Averty, M.H. Mathon, J. Nucl. Mater. 329–333 (2004) 333.
[9] B. Wilshire, T.D. Lieu, Mater. Sci. Eng. A 386 (2004) 81.
[10] T. Yamamoto, G.R. Odette, P. Miao, D.T. Hoelzer, J. Bentley, N. Hashimoto, H. Tanigawa, R.J. Kurtz, J. Nucl. Mater. (2007), doi:10.1016/j.jnucmat.2007.03.047.
[11] D.S. Gelles, J. Nucl. Mater. 233–237 (1996) 293.
[12] M.J. Alinger, G.R. Odette, D.T. Hoelzer, J. Nucl. Mater. 329–333 (2004) 382.
[13] S. Yamashita, S. Ohtsuka, N. Akasaka, S. Ukai, S. Ohnukiy, Phil. Mag. Lett. 84 (8) (2004) 525.
[14] M. Klimiankou, R. Lindau, A. Moslang, J. Nucl. Mater. 329–333 (2004) 347.
[15] H. Kishimoto, M.J. Alinger, G.R. Odette, T. Yamamoto, J. Nucl. Mater. 329–333 (2004) 369.
[16] M. Klimiankou, R. Lindau, A. Moslang, Micron 36 (2005) 1.
[17] M.K. Miller, D.T. Hoelzer, E.A. Kenik, K.F. Russell, Intermetallics 133&134 (2005) 387.
[18] M.K. Miller, K.F. Russell, D.T. Hoelzer, J. Nucl. Mater. 351 (2006) 261.
[19] S. Yamashita, K. Oka, S. Ohnuki, N. Akasaka, S. Ukai, J. Nucl. Mater. 307–311 (2002) 283.
[20] S. Yamashita, N. Akasaka, S. Ohnuki, J. Nucl. Mater. 329–333 (2004) 377.
[21] P. Pareige, M.K. Miller, R.E. Stoller, D.T. Hoelzer, E. Cadel, B. Radiquet, J. Nucl. Mater. 360 (2007) 136.
[22] M.K. Miller, D.T. Hoelzer, E.A. Kenik, K.F. Russell, Microsc. Microanal. 10 (Suppl. 2) (2004) 708.
[23] Y.L. Chen, A.R. Jones, U. Miller, Metall. Mater. Trans. A 33A (2002) 2713.